FEATURE ARTICLE

Computational Studies of DNA Photolyase

Christopher B. Harrison, Lauren L. O'Neil, and Olaf Wiest*

Department of Chemistry and Biochemistry, University of Notre Dame, Notre Dame, Indiana 46556-5670

Received: March 2, 2005; In Final Form: June 8, 2005

The electron transfer catalyzed (ETC) repair of the DNA photolesion cyclobutane pyrimidine dimer (CPD) is mediated by the enzyme DNA photolyase. Due to its importance as part of the cancer prevention mechanism in many organisms, but also due to its unique mechanism, this DNA photoreactivation is a topic of intense study. The progress in the application of computational methods to three aspects of the ETC repair of CPD is reviewed: (i) electronic structure calculations of the cycloreversion of the CPD radical cation and radical anion, (ii) MD simulations of the DNA photolyase and its complex to photodamaged DNA, and (iii) the structure and dynamics of photodamaged DNA. The contributions of this work to the overall understanding of the reaction and its relationship to the available experimental work are highlighted.

Introduction

Ultraviolet irradiation of DNA with light between 260 and 320 nm (UVB + UVC) induces formation of the *cis,syn* cyclobutane pyrimidine dimer (CPD, **2**) via a [2+2] cycloaddition.[1] This covalently linked dimer blocks cell replication and transcription, which compromises genetic information and ultimately leads to cell death or skin cancer.[2] Of the two principle repair mechanisms, humans possess the more common excision repair but lack the photoreactivation system found in many organisms where **2** is repaired via the enzyme DNA photolyase upon irradiation with light of wavelengths between 300 and 500 nm.[3] It should be emphasized that this enzyme mechanism distinguishes itself among enzymatic DNA repair mechanisms due to two unique features: First, this catalytic mechanism is directly triggered by light adsorption. Second, DNA photolyase utilizes light induced electron transfer catalysis to achieve a true repair as opposed to the base replacement as in the more common excision repair.

DNA photolyases are 454−614 amino acids in length and contain two noncovalently bound cofactors.[4] The first cofactor is the light-harvesting cofactor (LHC), which may, depending upon the organism, be either a deazaflavin (8-hydroxy-5-deazariboflavin, HDF) or a folate (methenyl-tetrahydrofolate, MTHF). As depicted in Figure 1, the LHC undergoes a $\pi \rightarrow \pi^*$ excitation upon absorption of light. Through a Förster-type energy transfer process, it excites the second catalytic cofactor, a redox active flavin, $FADH^-$, to its first excited state. The excited state now has a sufficiently low redox potential to effect an electron transfer to a cyclobutane pyrimidine dimer in DNA. Cycloreversion of the CPD radical anion restores the original bases. Back electron transfer finally then reduces the oxidized flavin radical, restoring it to its reduced, deprotonated form. This closes the cycle of the electron transfer catalysis (ETC) and effectively circumvents the symmetry forbidden thermal [2+2] cycloreversion.

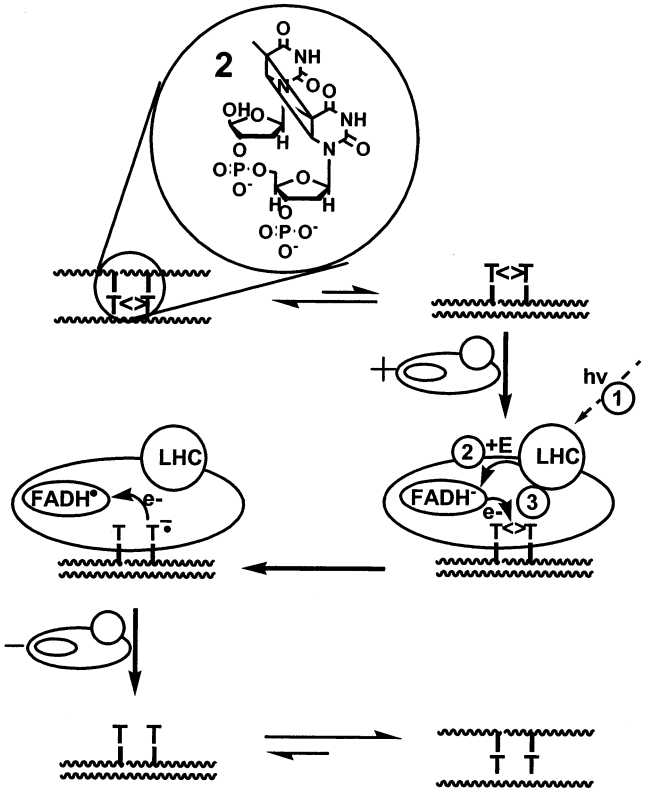

Figure 1. Scheme of repair of **2** by DNA photolyase.

Significant experimental effort has been directed at elucidating the details of this repair mechanism, which has been reviewed several times.[4−7] However, the unique mechanism and the difficulties associated with the enzyme−DNA substrate complex have placed significant limitations on experimental studies. Computational studies have therefore played an important role in deciphering inconclusive and even conflicting experimental evidence, providing insights into the mechanisms of repair at

* Corresponding author. E-mail: owiest@nd.edu.

10.1021/jp051075y CCC: $30.25
Published on Web 07/23/2005

Chris Harrison (middle) was born 68 years after T. H. White, to the hour. He received his first bachelors in English and Psychology in 2000. Soon realizing he was in fact no T. H. White, he completed his second bachelors in chemistry in 2002 from Western Kentucky University and began Ph.D. studies in physical organic chemistry at the University of Notre Dame with Olaf Wiest. The literary community has been eternally grateful. His current areas of interest include models and mechanisms of DNA photolyases, protein−protein/ligand interactions, reaction networks, small molecule ab initio reaction dynamics, computational method development, and enzyme reactions involving dynamic contributions, electron transfer, or proton/hydride transfers.

Lauren L O'Neil (right) was born in Syracuse, NY, in 1981 and raised in Weedsport, NY. She studied chemistry and biology at St. John Fisher College in Rochester, NY, and, during her undergraduate education, she worked in the lab of Prof. Kara L. Bren at the Univeristy of Rochester. In 2003, she joined the research group of Prof. Olaf Wiest where she has since been pursuing her Ph.D. in organic chemistry. Currently, her research is focused on the structure and dynamics of photodamaged DNA containing thymine dimers and the energetics and detection of base-flipping in such systems.

Olaf Wiest (left) was born in Germany and received his Ph.D. under the guidance of E. Steckhan at the University of Bonn in 1993. After spending two years as a Feodor-Lynen Fellow with K. N. Houk at the UCLA, he moved to the University of Notre Dame, where he was recently promoted to Professor in the Department of Chemistry and Biochemistry. His research interests center around electron transfer induced processes and their application in organic and bio-organic chemistry, as well as in computer aided molecular design. In his free time, he enjoys the Chicago Symphony Orchestra and good food.

an atomic level and models to guide experiment. Because the investigation of DNA photolyase is a very active research field and many important contributions of experimental results were communicated recently,[4−7] space constraints require that this review be highly focused on computational studies of DNA photolyase and can only mention a small portion of the vast number of experimental studies.

The computational investigations of DNA photolyase have predominantly been used to address two aspects of the problem. First, several of these studies were aimed at elucidation of the ETC repair mechanism of the CPD in the absence of the protein using electronic structure methods. Second, molecular mechanics methods were used to study the photodamaged DNA and its recognition by the enzyme DNA photolyase. Accordingly, this review will also be divided into two sections. The first section will review work directed at elucidation of the repair mechanism, and the second will focus on the structure and dynamics of CPD-containing DNA and its binding to DNA photolyase.

Mechanism of CPD Repair

Experimental studies on model systems showed that the ETC cycloreversion of CPD can proceed either via a radical-cation or a radical-anion mechanism (Figure 2). Although thermodynamic considerations,[4,8] kinetic isotope effects[9] and the presence of a reduced, deprotonated flavin in the active site of DNA photolyase[10] strongly suggest that the radical-anion mechanism is operative in the biological system, the exact details of both pathways have generated significant interest and have been studied computationally.

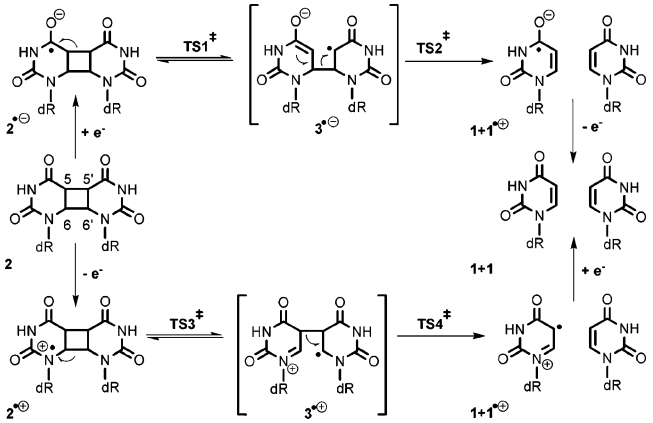

Figure 2. Reaction mechanisms of ET catalyzed repair of **2**.

Figure 2 summarizes the transition structures and putative intermediates of the cycloreversion of **2** through a radical cation or radical anion mechanism. The removal or addition of an electron to a CPD (either the thymine dimer **2t**, uracil dimer **2u**, or a related model system[11]) results in a weakening of the C6−C6′ or the C5−C5′ bond, respectively. Both pathways have been studied computationally with a wide range of methods. As will be discussed below, the choice of an appropriate computational method for the radical ions as well as a suitable model system are crucial for the validity of the results obtained.

Radical Cationic CPD Repair Pathway. Cycloreversion of **2** may be achieved through oxidative electron transfer catalysis, as shown in the lower pathway in Figure 2. The single electron oxidation of **2** by one of several possible oxidants[4−8] results in the radical cation, $\mathbf{2}^{\bullet+}$. Subsequently, cleavage of the C6−C6′ bond via TS3 leads to $\mathbf{3}^{\bullet+}$. Finally, cleavage of C5−C5′ yields one neutral pyrimidine, **1**, while leaving one radical cationic base, $\mathbf{1}^{\bullet+}$. Back electron transfer from $FADH^{\bullet 2-}$ then injects an electron into $\mathbf{1}^{\bullet+}$ leading to two restored pyrimidines, **1**.

Comparison of the UHF/6-31G* optimized structures of **2u** with that of the corresponding radical cation, $\mathbf{2u}^{\bullet+}$, revealed a lengthening of the C6−C6′ bond by 0.5 Å upon electron transfer.[12] The Hartree−Fock results strongly indicate the radical cationic pathway of cyclobutane pyrimidine dimer cleavage is stepwise with initial cleavage of C6−C6′ leading to a singly linked intermediate $\mathbf{3u}^{\bullet+}$. Starting from these results, CASSCF/6-31G calculations using a [3e,4o] active space[13] were used to map the reaction coordinate of radical cationic cleavage as depicted in Figure 2. Beginning from $\mathbf{2u}^{\bullet+}$, C6−C6′ cleavage exhibited a barrier of 0.3 kcal/mol, leading to $\mathbf{3u}^{\bullet+}$, which was −4.6 kcal/mol lower in energy than $\mathbf{2u}^{\bullet+}$. Subsequent C5−C5′ cleavage required 1.4 kcal/mol of activation energy, yielding $\mathbf{1u} + \mathbf{1u}^{\bullet+}$ with an overall reaction energy of −29.4 kcal/mol relative to $\mathbf{2u}^{\bullet+}$.

The radical cationic cleavage was also investigated with AM1[14] as well as UHF, MP2, and B3LYP using the 6-31G* basis set.[12b] Although the overall finding of a stepwise mechanism starting with cleavage of the C6−C6′ bond is common to all these studies, there are notable differences between the results from the different computational methodologies. UHF and B3LYP calculations predict that vertical ionization followed

by nuclear relaxation is exothermic by 18.4 and 16.7 kcal/mol, respectively. This is in contrast to the value of −38.5 kcal/mol predicted by MP2. Subsequent C6−C6′ cleavage, leading to **3u**$^{\bullet+}$, was calculated to be barrierless with $\Delta G^{\neq} < 1.0$ kcal/mol and exothermic by 27.4−32.3 kcal/mol via all methods except MP2, which predicted this step to be endothermic. These discrepancies are likely to be due to the well-known[15] problems of MP2 in treating spin contaminated open-shell species.

UHF predicted **3u**$^{\bullet+}$ to be separated from **1u**+**1u**$^{\bullet+}$ by transition structure **TS6**$^{\bullet+}$ for the C5−C5′ cleavage. B3LYP calculations were unable to locate this transition structure, suggesting the conversion of **2u** to **1u**+**1u**$^{\bullet+}$ may proceed with little or no activation energy. Although it is well-known that Hartree−Fock calculations frequently overestimate activation energies, the DFT results were in disagreement with the trapping of singly linked intermediates analogous to **3u**$^{\bullet+}$ in model systems.[16] The inclusion of aqueous solvent effects via SCRF/B3LYP/6-31G* calculations stabilized the charge localization that results from the formation of the smaller charge-carrying radical cation **1u**$^{\bullet+}$. As this charge localization increases along the reaction path between **2u** and **1u**+**1u**$^{\bullet+}$, the SCRF results become increasingly more exothermic than the gas phase data.[12b] However, solvent effects did not change the overall shape of the potential energy surface.

In DNA duplexes, hydrogen bonds to a uracil or thymine could lead to a deprotonation of the radical cation.[17] Removing the imide proton of N3 from **2u**$^{\bullet+}$, Rösch and co-workers investigated the effect of hydrogen bonding upon the radical cationic pathway using B3LYP/6-31G* and AM1.[18] Solvent effects for B3LYP calculations were estimated via scaling to AM1 gas phase and SCRF calculations. This solvation reduced barriers for C6−C6′ cleavage by 15.5 kcal/mol. Subsequent C5−C5′ cleavage was reduced by 3.5 kcal/mol. Overall, deprotonation of N3 exhibited rather high activation barriers in gas phase but this effectively disappears upon the inclusion of solvent effects, presumably due to the solvent stabilization of the resulting ions. Thus, deprotonation of **2u**$^{\bullet+}$ in DNA or in aqueous solution will not inhibit the repair reaction.

Radical Anionic CPD Repair Pathway. Unlike the radical cationic cycloreversion, which was studied for several different model systems, computational studies of the naturally occurring radical anionic pathway focused on the cyclobutane uracil dimer **2u**. In the radical anionic repair mechanism of **2u**, shown in the upper part of Figure 2, the addition of an electron to **2u** leads to **2u**$^{\bullet-}$, which subsequently cleaves C5−C5′ through transition state TS1 leading to **3u**$^{\bullet-}$ with an enolate on one pyrimidine moiety and an α-carbonyl radical on the other. Cleavage of C6−C6′ in transition state TS2 then yields an ion−molecule complex consisting of one neutral pyrimidine, **1u**, and one radical anionic pyrimidine, **1u**$^{\bullet-}$. Back electron transfer (BET) then restores the two neutral pyrimidines.

Rose and co-workers[19] investigated the relative energies of a concerted compared to stepwise mechanism using Hückel molecular orbitals calculations. In comparison to neutral pyrimidine dimers, a one-electron reduction of the dimer decreases the activation energy for splitting via nonsynchronous concerted and fully stepwise pathways. This decrease in activation energy is not obtained when energetics of the concerted pathway are calculated. Rose et al. thus argued that the injection of an electron into the dimer facilitates cycloreversion by stabilizing the system as it splits, offsetting the energetic demand of breaking a sigma bond.

Heelis calculated the enthalpic difference (ΔH_{spl}) between **2u** and **1u**+**1u** in attempts to assess the cyclobutane strain contribution to splitting.[20] Using the semiempirical PM3 method, the reaction enthalpy for the cycloreversion reaction was calculated to be −3.9 kcal/mol for the radical anion. For the case of the corresponding thymine dimer **2t**, the exothermicity of the reaction increases to 8.6 kcal/mol.

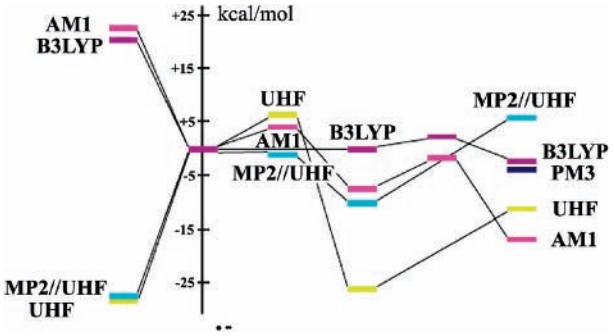

Figure 3. Potential energy diagram of radical anion repair mechanism.[21]

Figure 3[21] summarizes the results of the available computational studies of the reaction pathway at different levels of theory. Semiempirical AM1 calculations were used to investigate the mechanism of the radical anionic pathway for both the uracil, **2u**, and thymine dimers, **2t**. The C5−C5′ cleavage via TS1 was calculated to have an activation energy of 3.9 kcal/mol for **2u**$^{\bullet-}$ and to be exothermic by 7.5 kcal/mol with respect to the formation of the intermediate **3u**$^{\bullet-}$. Subsequent cleavage of C6−C6′ required 5.8 kcal/mol of activation energy to produce **1u**$^{\bullet-}$+**1u**, which was 13.6 and 21.1 kcal/mol lower in energy than **3u**$^{\bullet-}$ and **2u**$^{\bullet-}$, respectively. This overall reaction enthalpy is remarkably close to the experimentally deduced value of −21 kcal/mol.[22] In the thymine dimer **2t**, formation of TS1 required 4.7 kcal/mol of activation energy to produce **3t**$^{\bullet-}$, which was 18.5 kcal/mol more stable than **2t**$^{\bullet-}$. The C6−C6′ cleavage at TS2 required 5.3 kcal/mol of activation energy and yielded **1t**$^{\bullet-}$+**1t**, which was 17.4 and 30.6 kcal/mol more stable than **3t**$^{\bullet-}$ and **2t**$^{\bullet-}$, respectively. Using the self-consistent reaction field (SCRF) approach to describe solvation effects, these same pathways were calculated in hexane and DMF. In agreement with experimental findings that the quantum yield of repair decreases with increasing solvent polarity,[23] these calculations found the barrier for radical anionic cycloreversion to increase as a function of increasing polarity of the dielectric.

Subsequent work by the same group sought to address the discrepancies between the planar four-membered ring predicted by semiempirical methods and the puckered cyclobutane ring found in crystallographic studies of the uracil dimer[24] and the photodimer of 1,3-dimethylthymine[25] as well as ab initio calculations of the neutral and cationic dimers.[13,14] Attempting to address this known bias of semiempirical methods[26] and to study the structure and energetics of **2u** and the cycloreversion of its radical ion, **2u**$^{\bullet-}$, Voityuk and Rösch reevaluated their earlier semiempirical calculations of the radical anionic pathway using UHF/6-31G* and MP2/6-31G*.[27] UHF results were comparable to the earlier AM1 calculations and gave a barrier of 6.2 kcal/mol for TS1. The formation of the intermediate **3u**$^{\bullet-}$ was calculated to be exothermic by 25.1 kcal/mol relative to **2u**$^{\bullet-}$, indicating the stabilization of spin and charge through resonance. Though the second transition state, TS2, was not investigated in this study, the cleavage of the C6−C6′ bond in **3u**$^{\bullet-}$ leading to **1u**$^{\bullet-}$+**1u** was calculated to be 15.0 kcal/mol endothermic. The overall exothermicity was 11.3 kcal/mol upon thermal comparison of **2u**$^{\bullet-}$ and **1u**$^{\bullet-}$+**1u**. The results from the MP2 calculations were quite different from the earlier findings.

With an activation energy of −1.1 kcal/mol for TS1 after ZPE correction, initial C5−C5′ cleavage was calculated to be barrierless. However, **3u**•− was calculated to be only 10.3 kcal/mol more stable than **2u**•−. Again, TS2 was not calculated, but **3u**•− was found to be 16.2 kcal/mol more stable than **1u**•−+**1u**. Overall, MP2 results predicted the cycloreversion reaction from **2u**•− to **1u**•−+**1u** to be endothermic by almost 6 kcal/mol, in clear contrast to other computational methods as well as to experimental observation.[8,22]

The question of proton transfer to **2u**•− was investigated in an effort to determine if strong hydrogen bonds could impact the radical anionic cycloreversion of **2u**.[17] This phenomenon could occur through hydrogen bonding to the opposite adenine base or from aqueous solution. Modeled via protonation of the C4 carbonyl of **2u**•−, the cycloreversion of the resulting radical **2uH**• was calculated at B3LYP/6-31G* and AM1 in both the gas phase and water using the SCRF approach. This resulted in an increase in the energy necessary for the initial C5−C5′ cleavage and decreased the exothermicity by ∼10 kcal/mol, suggesting that this process is unlikely.

The unusually strong method dependence of the calculated electron affinity, overall thermochemistry, and mechanism summarized in Figure 3 suggests that the physical model underlying these gas phase calculations is not sufficient to provide a realistic representation of the cycloreversion process in condensed phase. The origin of this discrepancy becomes apparent upon consideration of the electronic structure of the pyrimidine radical anions. There is considerable experimental[28] and computational[29] evidence that formation of the dipole bound state of **1u** is exothermic in the gas phase, whereas the valence bound state is not stable.[30] A dipole bound (DB) state is characterized by an electron localized outside the molecular frame and toward the attractive field of the permanent molecular dipole moment.[31] Typically, this state is energetically accessible, provided the molecule exhibits a dipole moment greater than 2.5 D.[32] The second state, a valence bound (VB) state, has the extra electron localized to a valence shell of the molecule corresponding to its LUMO.

Experimental gas phase electron affinities (EAs) of uracil were determined by a number of different methods. By scaling half-wave potentials, Wiley et al. approximated the adiabatic electron affinity (EA_{adiab}) to be 18.44 kcal/mol.[33] The vertical electron affinity (EA_{vert}) was determined by electron scattering[34] and by resonant electron attachment[35] to be −5.07 and −7.06 kcal/mol, respectively, indicating a short-lived valence-bond state. In a different approach, by extrapolating EAs when water molecules are hydrogen bonded (stabilizing the VB state), Schiedt et al. estimated the electron affinity for the VB state to be 3.5 kcal/mol.[29] In comparison, dipole bound states were found experimentally[28a,d; 29] to have EAs of 2.14−1.96 kcal/mol.

These previous studies, with the exception of the work by Schiedt et al., examined the gas phase EAs and their applicability to the solvated enzymatic catalyzed reaction is unclear. As the dipole moment of the dimer increases, so too does the stabilization of the DB state. In the enzyme and in solution, hydrogen bonding from either water, complementary base pairing, or residues in the active site of DNA photolyase may stabilize the VB state. Hydrogen bonding of the C4 carbonyl function of **1** with water or other bases stabilizes the valence bound state and makes it energetically more favorable than the dipole bound state.[29] Because the dipole moment of **2** is higher than that of **1u**, the same situation will apply to **2**. It is therefore necessary to include both explicit and implicit solvent effects in the calculations.

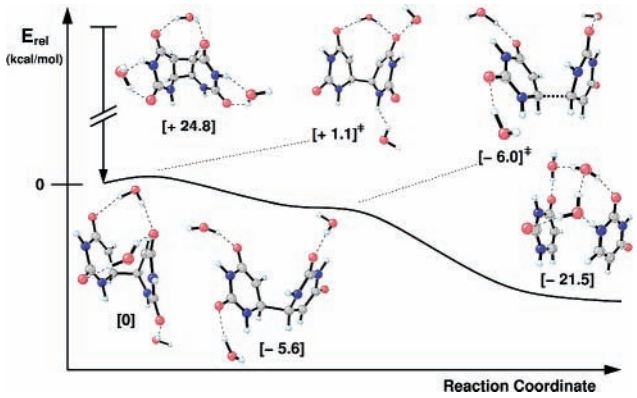

Figure 4. B3LYP/6-311++G**//B3LYP/6-31G* calculated pathway for cycloreversion of **2u** in theozyme.

In analogy to the computational investigations of the electron affinity of pyrimidines using explicit solvent molecules,[36] the cycloreversion of **2u**•− hydrogen bonded to three water molecules, in a theozyme fashion,[37] was studied at the B3LYP/6-311++G**//B3LYP/6-31G* level of theory.[38] In the absence of the theozyme, the results were in accordance with earlier calculations by Rösch.[26] Upon inclusion of the theozyme, the results summarized in Figure 4 were obtained. The hydrogen bond to the C4 carbonyl has a dramatic effect on the mechanism and relative energetics of the reaction. The electron attachment is now exothermic by 24.8 kcal/mol and proceeds via a valence bound state. This initial ionization results in a lengthening of the C5−C5′ bond from 1.6 to 2.5 Å, which was rationalized as a delocalization of the singly occupied C4−O π* orbital into the C5−C5′ σ* orbital. Crossing of the first barrier then corresponded to a C5−C6−C6′−C5′ dihedral change from 30° in the anion to −71° in the intermediate where C5−C5′ has been completely cleaved but C6−C6′ has not. Subsequent C6−C6′ cleavage occurs, after correction for zero-point energy, without a barrier. The calculated overall reaction energy of −21.5 kcal/mol is in quantitative agreement with the experimental value of −21 kcal/mol.[22] Though the overall exothermic reaction energy with one water is less than the reaction energy without it, the number of waters present does not significantly influence the activation energy.[21] This reaction, which was previously predicted to be stepwise with a substantial barrier in the second step, is in the presence of hydrogen bonding solvent molecules effectively barrierless; i.e., the barriers are lower than the thermal energy at room temperature. This is in agreement with the experimental observation that, unlike the case of the radical cationic reaction, no single intermediate can be trapped in the case of the radical anionic reaction.[39] The quasi-concerted mechanism can be rationalized by stabilization of the developing negative charge on the C4-carbonyl by hydrogen bonding, which can only be represented by using explicit solvent models. As will be discussed later, the crucial hydrogen bond could be provided by residues in the active site of the enzyme. These results demonstrate the necessity of constructing a proper model system for not only calculations of the electron affinity but also calculations of the relevant mechanism.

Excited States of Flavin and the Thermodynamic Cycle for CPD Repair. For a complete consideration of the thermodynamics of the light-driven repair reaction, inclusion of the energetic contributions from the two cofactors, FADH and the LHC, are necessary. Durbeej et al.[40] studied the thermochemistry of the electron transfer reaction. Using time dependent DFT methods (TD-B3LYP/6-311G(2df,p)//B3LYP/6-31G(d,p)), the

TABLE 1: Relative Energies of Species Involved in the Repair of 2[40]

species	relative energy (kcal/mol)
$FADH^-$ (S_o)	0
$FADH^\bullet$	42.9
$^1FADH^-$ (S_1)	61.1
1 (T)	0
$1^{\bullet-}$	0.07
$1^\bullet$	202.6
2 (TT)	0
$2^{\bullet-}$	−20.2
$2^\bullet$	196

$S_0 \rightarrow S_1$ excitation for $FADH^-$ was calculated to be endothermic by 61.1 kcal/mol, as shown in Table 1. Electron transfer from $FADH^-$ to **2** yields $\mathbf{2}^{\bullet-}$ and $FADH^\bullet$, a step that is exothermic by 18.2 kcal/mol. Direct regeneration of the catalytic $FADH^-$ from $FADH^\bullet$ is thus 42.9 kcal/mol exothermic.

These calculations provide the basis for a computational investigation of the preference of the radical anionic over the radical cationic pathway. As discussed earlier, thermodynamic considerations indicated that the radical anionic pathway operates in the enzyme, but a radical cationic cycloreversion is feasible and leads to the same products. Using the same methodology, the adiabatic electron affinity and ionization potential of **2t** was calculated to be −20.2 and 196 kcal/mol, respectively. Incorporation of the energies for various excited flavin species only increases the difference between the energies of the $\mathbf{2t}^{\bullet-}$ and $\mathbf{2t}^{\bullet+}$, as shown in Figure 5. The driving force of the reductive electron transfer leading to $\mathbf{2t}^{\bullet-}$ is calculated to be −38.5 kcal/mol, whereas the formation of $\mathbf{2t}^{\bullet+}$ is 231.8 kcal/mol uphill. Under the assumption that the calculated energies can be compared to the experimentally determined free energies, these results can be compared to the observed values of $\Delta G(\mathrm{Red})_{exp}$ of −29.9 kcal/mol for the radical anion mechanism.[5] This assumption was justified by earlier results that the entropic contributions for the cycloreversion are small in a constrained environment such as the enzyme active site.[27] Likewise, the reported $\Delta G(\mathrm{Ox})_{exp}$ of 43.1 kcal/mol for the radical cation mechanism differs substantially from the calculated $\Delta G(\mathrm{Ox})_{calc}$ of 231.8 kcal/mol. Although the calculations, in agreement with experiment, strongly favor the reductive ET with a calculated $\Delta\Delta G_{calc} = 270.3$ kcal/mol, this greatly overestimates the experimental value of $\Delta\Delta G_{exp} = 73.0$. Although the radical anion system exhibits less deviation from the experiment value than the radical cation system, both systems' deviations from experiment are significant. This discrepancy between theory and experiment was attributed to the absence of the LHC in the calculated system.

To improve on these results, a more complete thermodynamic cycle was constructed by incorporation of the LHC cofactor, as shown in Figure 6. Following an $S_0 \rightarrow S_1$ excitation, the excited state of the LHC undergoes an energy transfer to the $FADH^-$ that is 15.5 to 16.2 kcal/mol exothermic. Electron transfer from the excited singlet state of the FADH anion ($^1FADH^-$) to **2** results in formation of $FADH^\bullet$ and $\mathbf{2}^{\bullet-}$ as discussed above. This is followed by dimer cleavage, yielding **1** and $\mathbf{1}^{\bullet-}$. BET from $\mathbf{1}^{\bullet-}$ to $FADH^\bullet$ then reduces the flavin to $FADH^-$ and restores **1**, a process calculated to be 44.7 kcal/mol exothermic, in acceptable agreement to the experimental value of 49.7 kcal/mol.[5] Although there are several instances of error cancellation, this calculated thermodynamic model predicts the cycle to be 22.1 kcal/mol exothermic, in excellent agreement with the experimental value of 22.2 kcal/mol.

Although the catalytically active form of the flavin is the reduced, deprotonated form, $FADH^-$, the flavin radical $FADH^\bullet$

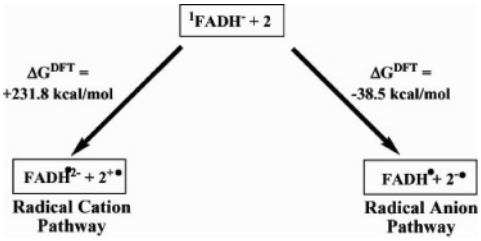

Figure 5. Free energy difference between radical cationic and radical anionic pathways.[40]

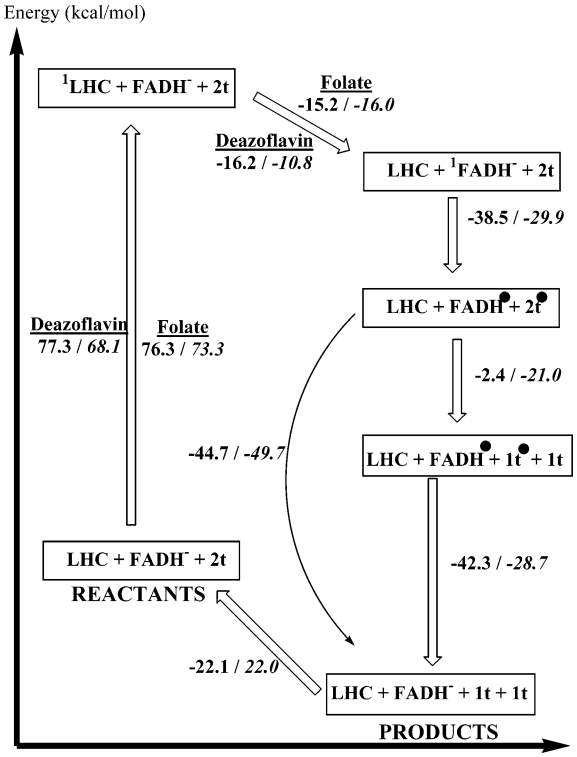

Figure 6. Thermodynamic cycle for the major steps of the radical anionic repair mechanism in DNA photolyase. Calculated values are in plain text; experimental values are in italics.[40]

exists as an inactive resting state that can be reactivated by irradiation with visible light. Site directed mutagenesis studies and time-resolved spectroscopy suggests that Trp^{306} is the electron donor in this process[41] even though it is ∼15 Å away from the flavine.[10a] This long-range radical transfer leading to a photoreactivation has been studied computationally.

Calculation of the electrostatic free energies of the different charge separated states in the enzyme using a Poisson−Boltzmann approach[42a] indicate that the process is overall exothermic, even though the exact value is dependent on the assumptions for the unknown redox potential of $FADH^\bullet$. The reaction assumes a stepwise ET along the conserved triad of tryptophanes 382, 359 and 306 and is terminated by deprotonation of the radical cation of Trp^{306}. This model for the long-range ET is in agreement with previous computational predictions based on the interatomic tunneling method that calculated the electron flow within the extended Hückel approximation.[42b]

Recognition and Binding of Photodamaged DNA to DNA Photolyase

The structure of DNA photolyase from *E. coli* (PDB ID: 1dnp) shows five parallel β-strands, 20 α-helices, and five short 3_{10} helices that form three domains.[10] Two of these domains are separated by a "hole" surrounded by a flat protein surface.

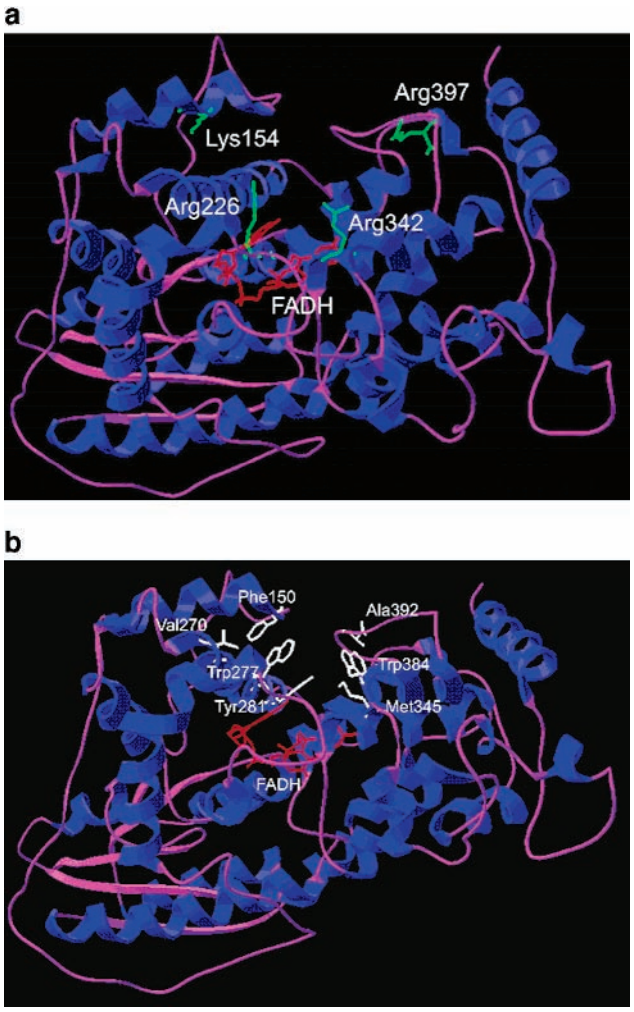

Figure 7. Crystal structure of *E. coli* DNA photolyase showing FADH in red. (a) positively charged residues, Arg^{226}, Arg^{342}, Arg^{397}, and Lys^{154} in green, (b) hydrophobic binding pocket residues, Phe^{150}, Val^{270}, Trp^{277}, Tyr^{281}, Met^{345}, Trp^{384}, and Ala^{392} in white.

This hole contains the FADH cofactor and is the CPD binding site with size complementarity of the hole to the dimer. This hole is characterized by a positively charged rim, consisting of Arg^{226}, Arg^{342}, Arg^{397}, and Lys^{154}, and a hydrophobic binding pocket, consisting of Phe^{150}, Val^{270}, Trp^{277}, Tyr^{281}, Met^{345}, Trp^{384}, and Ala^{392} (Figure 7a,b). In addition, the three-dimensional structures of photolyases from *Anacystis nidulans* and *Thermus thermophilus* with a thymine bound to the active site have been reported.[43] The rms deviations of the C_α atoms common to the CPD photolyases from *T. thermophilus/E. coli*, *T. thermophilus/A. nidulans*, and *E. coli/A. nidulans* are 1.54, 1.60, and 1.12 Å, respectively. Due to this high structural similarity, it can be expected that studies on one structure will be transferable to other photolyases.

Computational chemistry, especially force field and molecular dynamics methods, have been used extensively to understand the peculiarities of this enzyme structure and to use the structural information to provide insights into the recognition of the photodamaged DNA by the enzyme and the electron transfer catalyzed repair process. It can be expected that the results from this work, combined with the very recently elucidated three-dimensional structure of an enzyme−substrate analogue complex of *A. nidulans* photolyase complexed to a model of photodamaged DNA,[44] will help to solve the many unanswered questions regarding the mechanism of recognition and repair by this unique enzyme.

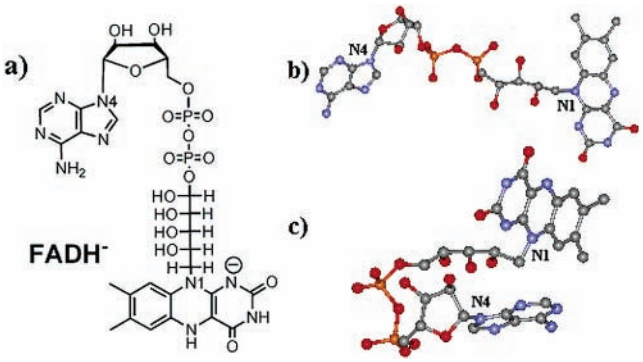

Figure 8. FADH structures: (a) schematically, with N1 and N4 labeled; (b) representative I-shaped structure (PDB ID: 1buc); (c) U-shaped structure from *E. coli* DNA photolyase (PDB ID: 1dnp).

TABLE 2: Structural Features of FADH

	N1−N4 distance (Å)
crystal structure[10a]	5.9
energy minimization of crystal structure **2**	8.1
MD simulation of water-solvated FADH	7.8
mean value obtained from MD simulation of enzyme complex	6.1

Cofactor Binding to DNA Photolyase. The repair reaction catalyzed by DNA photolyase is dependent on binding of both the cofactor(s), FADH and/or MTHF,[4] and the species to be repaired, a thymine dimer, T<>T. FADH consists of four components, the photoactive isoalloxazine, ribose, phosphate, and adenosine, as shown in Figure 8a. Experimentally determined FADH conformations of 32 flavoproteins in the Protein Data Bank show mostly I-type conformations, i.e., extended or linear structures in which the N1(of the isoalloxazine)−N4(of the adenine) distance is approximately 13−16 Å, as shown in Figure 8b. This is due to the binding of only one moiety of the FADH by the enzyme, leaving the other moiety solvent exposed. The binding site for the FADH in *E. coli* DNA photolyase is not solvent exposed and the crystal structure reveals that the FADH cofactor is bound in an uncommon U-type conformation with a N1−N4 distance of ∼6 Å, as shown in Figure 8c.

Molecular dynamics (MD) simulations were performed on FADH in the gas phase, in water and as a part of the FADH−enzyme complex.[45] The results of the simulations of FADH show several different conformations within 8 kcal/mol of the minimum and with N1−N4 distance ranges of 4−14 Å. This is indicative of the flexibility of free FADH under these conditions. Among the conformations encountered in the MD simulations following energy minimization was the U-type conformation, which was identified as a local minimum. The crystal structure of FADH in the *E. coli* photolyase[10] was energy minimized for comparison to both the crystal structure and the U-shaped conformation of FADH obtained during the course of the MD simulation. As shown in Table 2, the calculated conformations differ from the crystal structure in the N1−N4 distance by 1.0−2.1 Å.

The simulations of FADH and the enzyme−FADH complex included explicit waters, which the authors assumed provided a reasonable model for solvation. The major difference between the solvated and nonsolvated structures is the N1−N4 distance, which decreased from 8.1 to 7.8 Å. The resulting solvated structure of FADH is structurally more similar to that of the FADH in the crystal structure of photolyase. The MD simulations of the enzyme−FADH complex were run for up to 1.2 ns. During that time the FADH stayed in the U-shaped

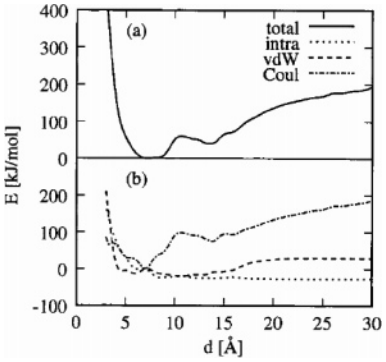

Figure 9. Interaction energy of the enzyme and model dimer at distance *d* above the bottom of the binding pocket, normalized to the value at $d = 6$ Å.

conformation with an average N1−N4 distance of 6.1 Å. The FADH was also noted to be quite inflexible with a RMS of 1.2 Å during the 50−300 ps time frame. In general, the results for FADH show that the cofactor fits well into the binding pocket and exhibits structural parameters very close to those observed in the crystal structure. These studies show that the deeply buried FADH binding site is optimized to hold the cofactor in an unusual, but well-defined, conformation. As will be discussed later, this unusual conformation is likely to play an important role in the electron transfer process.

Binding of Thymine Dimer to DNA Photolyase. The binding of a thymine dimer **2t** to the enzyme active site to predict the structure of the enzyme−substrate complex has also been widely studied. From these studies, two models for the enzyme−substrate complex have been developed. The major difference between these two binding models is in the distance between the dimer and the FADH. The first model, developed independently by Rösch and co-workers[46] and also Wiest and co-workers,[47] describes a binding mode in which bound **2** has a significant distance to the redox active cofactor, FADH. The second model, developed by Stuchebrukhov and co-workers,[48] suggests that the distance between the dimer and the FADH is much smaller and the dimer is in close van der Waals contact with the FADH. As a result, the interactions between **2** and the enzyme differ substantially between the two models.

The first of the two binding models has been studied using MD simulations of both model dimers and single-stranded DNA. Rösch and co-workers studied the binding of a mixed uracil-thymine pyrimidine dimer, **U**<>**T**, as well as a **U**⟨*p*⟩**T** DNA fragment, consisting of the dimer and a single ribophosphate unit linking the two pyrimidines.[45] The use of a **U**<>**T** dimers was prompted by the previous use of these dimers in substrate dependent repair studies.[49] The binding pocket was examined by fixing all atoms of the enzyme and FADH to their position in the crystal structure and performing a stepwise reduction of the distance between the model dimer and the bottom of the active site pocket from 30 to 3 Å. At each step, the geometry of the dimer was optimized and the total energy and its contributing factors were plotted against the distance, as shown in Figure 9. In this model, there is a low-energy region ∼12−14 Å above the pocket region. Further reduction of this distance produces an energy barrier (∼8−12 Å above the bottom of the binding pocket). The second energy minimum is found at ∼6 Å, showing close contact between the dimer and the cofactor at the bottom of the pocket.

Molecular dynamics (MD) simulations using the AMBER force field[50] were also performed on the enzyme containing the FADH cofactor and the model dimers with explicit solvent. The results of the MD simulations showed that the distance between

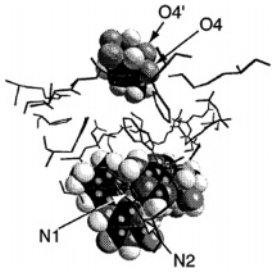

Figure 10. Snapshot of MD simulation of enzyme, cofactor and substrate showing the **U**<>**T** dimer in enzyme active site (only adjacent amino acids are shown for clarity).

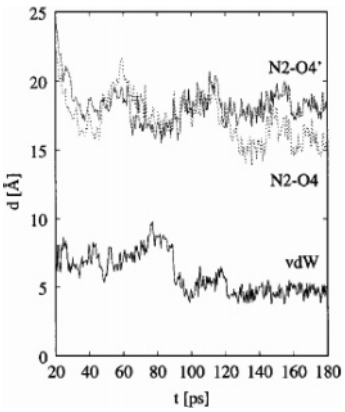

Figure 11. Minimum van der Waals distance, *d*, between the bare dimer, **U**<>**T** and FADH as a function of simulation time. Distance between N2 of FADH and O4 and O4′ of the dimer as a function of simulation time are also shown.

the dimers and the cofactor, essentially the penetration depth of the dimer in the active site, is largely dependent on steric interactions, as shown in Figure 10. Figure 11 shows the van der Waals distance, *d*, between FADH and **U**<>**T** as a function of simulation time. The minimum van der Waals distance between the dimer and the sugar moiety of the cofactor FADH is ∼7 Å in the 20−80 ps time period after which it drops to ∼5 Å and remains close to this value until the end of the simulation. Also shown is the distance between the N2 of the FADH and the O4 of the model dimer, which is ∼15 Å at the minimum. For the case of the model dimer containing the phosphate linker, **U**⟨*p*⟩**T**, these relatively close contacts were not found. The minimum distance between the dimer and the sugar moiety of the cofactor FADH increases to ∼9 Å. The authors concluded that this large distance, which might be even larger in the case of a larger DNA strand, makes a direct electron transfer unlikely.

This model is similar to the one from a similar study performed by Wiest and co-workers, which used not only dinucleotide model dimers but also single-stranded and duplex DNA.[47] The binding of a dinucleotide **2t** was studied using a manual docking procedure, and approximately 30 docked orientations, which converged upon energy minimization to two distinct structures, were considered. Molecular dynamics simulations were then run on the lowest energy structures. The lowest energy structure shows several interesting features (Figure 12).

The phosphate backbone of the dimer rests on the positively charged rim of the binding site (Arg^{342}, Arg^{397}, and Lys^{154}) whereas the T<>T dimer is in contact with two tryptophans (Trp^{277} and Trp^{384}) that provide a hydrophobic binding pocket. In addition, Trp^{384} is positioned to provide the hydrogen bonding interaction found to be crucial for the reaction mechanism as discussed earlier. In accordance with the model developed by

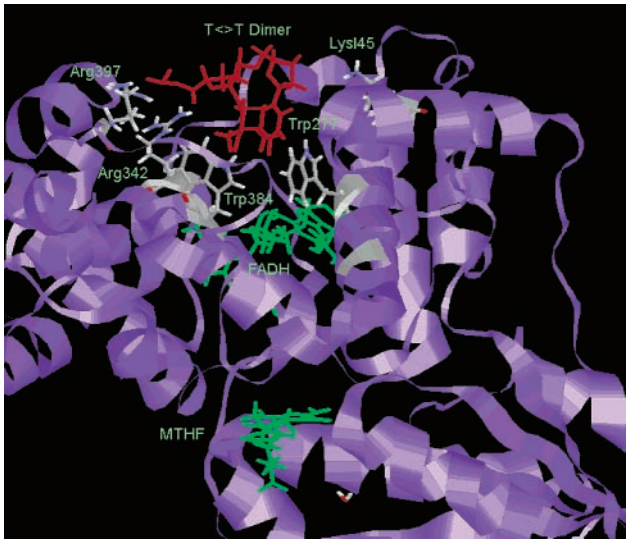

Figure 12. Model of enzyme−substrate complex with cofactors in green, **2u** shown in red.[47]

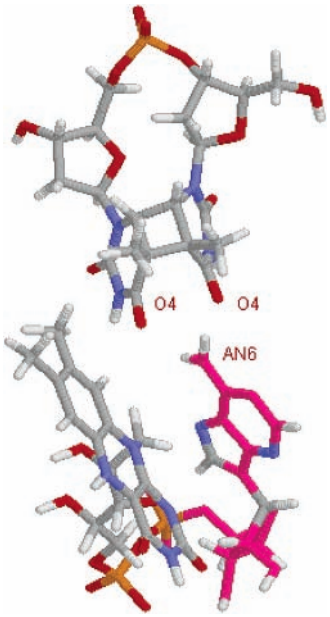

Figure 13. Predicted relative positions of **2t** and FADH from ref 48a.

Rösch and co-workers, no close contacts between the dimer and FADH are observed. The smallest observed distance between the isoalloxazine ring of the FADH, the redox active portion, and **2** is ∼10 Å. Recent EPR and ENDOR experiments are most consistent with a large distance (>6 Å) between the isoalloxazine portion of the FADH and **2t**,[51] and the analysis of the X-ray structure of a thymine bound to the *T. thermophilus* photolyase concludes that the "inner part of the hole is too small for two thymine bases".[43]

The binding of a DNA single-strand (CGAAT<>TCGC) containing a **2** in its normal as well as in a "flipped-out" position was also studied using the same procedure. This resulted in two structures that again differed in the 3′→5′ directionality of the ssDNA. However, only the structure shown in Figure 12 rationalized the alkylation studies by Husain et al.[52] In these studies, the observed salt bridges between negatively charged phosphate groups of the DNA backbone with the positively charged rim (Arg^{397}, Arg^{342}, and Lys^{154}) would be interrupted by alkylation. The asymmetry of the salt bridges calculated correlates well with the fact that alkylation of any of the three phosphates 3′, but not 5′, to **2t** disrupts binding. These interactions, as well as that of Arg^{226} and the phosphate group 3′ to **2t**, are not observed in the dinucleotide case and move the dimer even further away from the redox active portion of the FADH. On the basis of these results, only one of the two possible 3′→5′ orientations was chosen for further studies. The alternative model that reverses the 3′→5′ directionality of the DNA has been proposed for the case of the yeast photolyase[53] and is in better agreement with more recent NMR data for photolyase from *T. thermophilus*[54] as well as the X-ray structure of a model system of photodamaged DNA bound to the *A. nidulans* photolyase.[44]

To combine these backbone interactions with the ones from the single strand and dinucleotide models previously calculated, the dimer in the single strand of DNA has to "flip-out" of the based-stacked helix position into the active site. This base flipping is well established for the case of DNA photolyase as well as many other DNA repair enzymes.[55,56] The "flipped-out" model was again manually docked into the active site and molecular dynamics simulations were performed. The interactions between the phosphate backbone and the positively charged rim are still present and the dimer is buried deeper in the pocket than in the base stacked simulations. However, the distance between the dimer and the redox active isoxazole moiety of the FADH cofactor is still larger than in the dinucleotide simulations.

The second of the binding models was developed by Stuchebrukhov and co-workers with a focus upon explanation of the experimentally determined rate of electron transfer.[48] Binding of dinucleotide dimers to *E. coli* photolyase was studied using DOCK 4.0. Calculation of the electronic coupling as expressed through the transfer matrix element for the donor and acceptor states of the enzyme−substrate complex was used in addition to the energy scoring function to evaluate the structures. The results of the docking using a rigid ligand receptor show conformations with a distance between the dimer and the flavin between 2.5 and 5.5 Å are the closest to the electronic coupling deduced from the experimentally determined rates. The structure in which there is the largest coupling strength between the dimer and flavin is found with a distance between the two of 2.8 Å. This structure was then used as a starting point for the MD simulations performed.

During the 1 ns production run time of the MD simulation the dimer moved slightly out of the pocket as compared with the position of the docking structure. A representative snapshot structure is shown in Figure 13. As can be seen, the smaller model system used in these calculations omits several of the surface-exposed "bottleneck" residues that were found by Rösch et al.[46] to block the closer approach of the dinucleotide to the redox active cofactor. This leads to the key difference between this model and the one discussed earlier is that distances between the carbonyl groups of the dimer (C4═O4) and the $-NH_2$ (AN6) of the FADH cofactor are ∼2.9 and ∼3.9 Å, compared to the docking structure distance of ∼2.4 and ∼2.6 Å. The transfer matrix element was calculated approximately every 20 ps along the trajectory using only the FADH, dimer and adjacent water molecules as shown in Figure 14.[57] This calculation assumes that the protein matrix does not influence the process of electron transfer. The maximum value for the matrix element was found to be 33 cm^{-1}, and the root-mean-square of the transfer matrix element was found to be 6 cm^{-1} ±5 cm^{-1} for **2t**. Comparison of the computed electronic coupling T_{DA} to experimental values

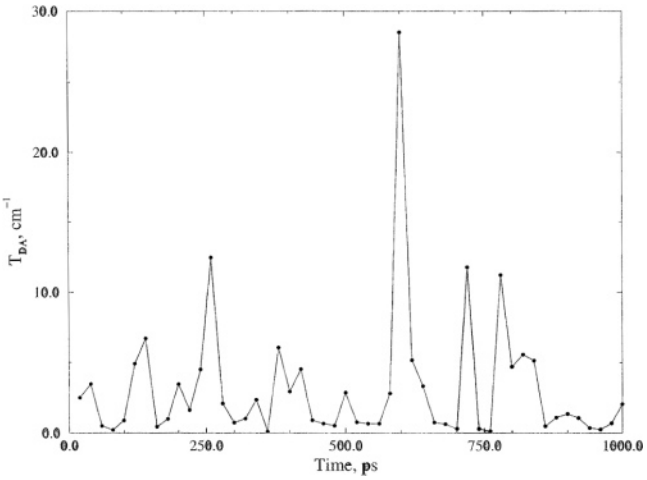

Figure 14. Calculated transfer matrix element along the dynamics trajectory.[48]

was achieved by using the rate expression for nonadiabatic electron transfer

$$k = \frac{2\pi}{\hbar}|T_{DA}|^2\rho_{FC} \quad (1)$$

The Franck−Condon factor ρ_{FC} is given in the classical approximation by

$$\rho_{FC} = \sqrt{\frac{1}{4\pi\lambda k_B T}}\exp\left(-\frac{(\lambda + \Delta G_0)^2}{4\lambda k_B T}\right) \quad (2)$$

Stuchebrukhov and co-workers estimated the reorganization energy term, λ, to be in the range 0.5−1 eV for a protein and, to estimate an upper limit for the Franck−Condon factor, ρ_{FC}, set the exponential portion of the equation equal to 1. Using their calculated Franck−Condon factor, ρ_{FC}, and the experimentally determined rates of 100 ps^{-1} at 275 K and 400 ps^{-1} at 90 K, it was concluded that the value of the transfer matrix element that is in agreement with experimental data must be at least 10 cm^{-1}. The examination of structures that give sufficiently large transfer matrix elements showed a close contact, less than 3 Å, between the dimer and the adenine portion of the cofactor. This would indicate that the electron transfer event from the redox active isoalloxazine portion of the FADH and the dimer is mediated by the adenine of the FADH.

It is interesting to compare the two models that were developed using two very different computational approaches. Both computational models and the available experimental data[58,59] agree that the CPD has to flip out of the DNA duplex to enter the active site of the photolyase. The models developed on the basis of the simulations done by Rösch, Wiest, and their co-workers can be compared to a bottle, the entrance to the active site is likened to the bottleneck and the dimer is the stopper. The stopper is unable to move into the bottle because the bottleneck is too narrow. Major reorganization of residues to allow a closer contact between the CPD and the FADH at the bottom of the active site might be possible but are beyond the time scales accessible by the MD methods used. Thus, the shape of the active site precludes any close contact between the cofactor and the substrate. This binding model is consistent with ESR studies of substrate binding to DNA photolyase. The matrix ENDOR signals show no change upon substrate binding, indicative of a distance between the dimer and the FADH of greater than 6 Å, which is in agreement with the 5.5−8 Å distance indicated by Stark effect measurements.[51,60] These models are also consistent with recent measurements of the paramagnetic relaxation enhancement (PRE)[61] of photodamaged DNA bound to *T. thermophilus* photolyase, which predicted a distance of 16 ± 3 Å between the FADH and the CPD.

The binding model developed by Stuchebrukhov and co-workers is in very good agreement with the X-ray structure[44] in that it predicts a close contact between the dimer and the cofactor of ∼3 Å, mediated by a bifurcated hydrogen bond between the (C4═O4) carbonyl of the CPD and the $-NH_2$ group of the adenine portion of the cofactor. This position of the adenine provides the hydrogen bonding to the C4 carbonyl that was found to be crucial for the stabilization of the valence bound radical anion[21,38] and provides the rationalization for the unusual conformation of the FADH.[45] Within the limits of the approximations made, the predicted electronic coupling is in agreement with the experimentally observed rate of electron transfer and suggests an indirect electron transfer involving the adenine portion of the FADH.

The differences between the two computational models are representative of the apparent contradiction between the experimental ESR and NMR results on one hand and the rate constants and X-ray results on the other. The atomistic description provided by the computational models thus forms the basis for future studies that could reconcile the experimental data and provide a definitive picture of the mechanism for damage recognition and repair by CPD photolyase.

Dynamics of Damaged DNA. All available experimental and computational studies of CPD photolyases agree that DNA repair requires a base flip of the lesion out of its normal position in the DNA duplex into the active site of the enzyme. Although the exact timing between base flipping and binding of the photodamaged DNA is not known, the conformational behavior, recognition, and binding of photodamaged DNA strands is inherently a part of the overall repair mechanism and needs to be more fully understood. Computational studies of damaged DNA have been performed by Kim et al.,[62] Miaskiewicz et al.,[63] and Spector et al.[64] Kim et al. performed energy minimizations using the AMBER force field parameters of Weiner et al.[65] and Rao et al.[66] on a DNA decamer by gradually releasing restraints placed on angles and distances and minimizing the resulting structure in an attempt to remove the bias toward the initial structure. The two most recent studies[61,62] reported MD simulations on thymine dimer-containing DNA, the former using a dodecamer and a 500 ps production time and the latter using a decamer and an 800 ps production time. Both simulations were performed using AMBER and the force field of Cornell et al.[63] The simulations contained sodium counterions and TIP3P water boxes of different sizes. Both of the PME simulations were performed using SHAKE bond constraints, a 9 Å Lennard-Jones cutoff, and a 2 fs time step at 298 K. Representative structures from the study performed by Kollman and co-workers are shown in Figure 15.

DNA containing a thymine dimer, as shown in Figure 15, is distorted from its native conformation, the global bend is greater and a kink is introduced. The major difference between the calculated structures is the global bend and the resulting kink. The kink angle for the Kim et al. structure was calculated to be approximately 30°. The results of the MD simulations were analyzed using CURVES[67] to determine the global bend and kink angles, among many other parameters, of the various structures. The global bend and kink angle for the Miaskeiwicz et al. structure were calculated to be 11° (relative to the native duplex). Another interesting feature of this structure was the disrupted hydrogen bond between the N−H of the 5′-thymine

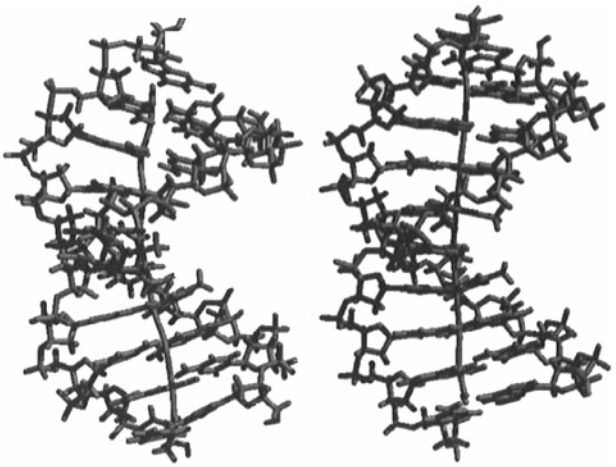

Figure 15. Comparison of average structures for photodamaged (left) and native (right) $d(CGCATTACGC)_2$ duplex from 800 ps MD simulations.[62]

of the dimer and the N of the adenine on the opposite strand. The bond was stretched to 2.5 Å and the N−H−N angle was 125°. Disruptions in base stacking were also observed. The tilt and roll of the bases of the dimer, caused by the presence of the cyclobutane linkage, make a parallel stacking of the bases impossible. The kink angle for the structure was calculated by Spector et al. to be 14° (relative to the native duplex). An X-ray structure of a DNA duplex containing **2**[68] showed a kink angle of 15°, in "remarkably close agreement" to the values calculated.[61,62] Earlier studies using NMR, electron microscopy, and gel shift methods had been less conclusive and reported kink angles between 5° and 30°.[69]

As the dimer must be "flipped-out" of the duplex to be repaired by DNA photolyase, the dimer flipping process is a very important aspect of the subject of dimer repair. Not only studies of the base flipping process but also continuations of the studies on dynamics of damaged DNA are crucial to the understanding of recognition and repair of thymine dimer-containing DNA. On the basis of the distortions induced by the presence of **2t** in the duplex, it can be expected that base flipping will be facilitated compared to the undamaged DNA. However, very few computational investigations of dimer flipping have been performed to date and the structure and dynamics of the flipped-out structures are unknown. One of the few available studies investigated the flipping of the adenine opposite the **2t** lesion,[70] which was found experimentally to be in a flipped-out position upon binding to the T4 endonuclease V.[71] Using a potential of mean force approach, the free energy required for base flipping of the A was calculated to be ∼5.4 kcal/mol. No studies of the flipping of **2t** from a DNA duplex have been reported yet and the energetic requirements and structural effects of this process are still unknown.

Summary and Conclusions

The computational studies of DNA photolyase have provided numerous insights into the structure and mechanism of this unique DNA repair reaction. Electronic structure calculations of the radical cationic reaction predict a stepwise pathway involving a C5−C5′ linked intermediate, which is in agreement with experimental trapping studies. Inclusion of the excited states of the cofactors from the enzyme into the calculations reveals that the oxidative pathway is greatly disfavored over the reductive repair mechanism, even though the actual value is significantly overestimated. Quantum mechanical calculations of the radical anionic pathway in the gas phase using a variety of methods do not offer a consensus, and inclusion of explicit hydrogen bonding stabilizes the chemically relevant valence bound radical anion over the dipole bound state. This model predicts an essentially barrierless cycloreversion that is exothermic by 21.5 kcal/mol, which is in good agreement with the experimentally determined value of 22.2 kcal/mol and the fact that no intermediate could be trapped in this reaction. Comparison of the results from these studies reemphasize the importance of choosing a proper model system as well as a suitable computational method that is able to handle the charged, open shell species involved in the reaction pathways.

Studies of substrate recognition and binding to DNA photolyases have utilized primarily molecular mechanics methods. Binding of the essential cofactor, FADH, to DNA photolyase takes place with the cofactor in an unusual, U-type, conformation. This conformation was studied using MD simulations and it was concluded that, though unusual, the FADH conformation is well-defined and the binding site is optimal for such a conformation. The binding of thymine dimers to DNA photolyases was also studied extensively computationally, and two different binding models have been predicted. In the model developed independently by Rösch and co-workers[45] and Wiest and co-workers,[47] **2** is ∼10 Å away from the redox active FADH cofactor at the bottom of the active site and no direct contact predicted. This model is in agreement with the results from ESR and NMR studies,[57,58] that predict large distances between the **2** and the FADH. In the model developed by Stuchebrukhov and co-workers,[48] the dimer and adenine portion of the FADH are within hydrogen bonding distance of each other, predicting an indirect pathway for the electron transfer. This model is in excellent agreement with a recent X-ray structure of photolyase from *A. nidulans* bound to a DNA strand containing a model of **2t**.[44] It can be expected that the two computational models can help to resolve the apparent contradiction between the spectroscopic and crystallographic results in analogy to the excellent results that were obtained for the predicted structure of the photodamaged DNA as well as the good agreement between computational and experimental results for the reaction mechanism.

The combination of computational and experimental studies of DNA photolyase, including mechanism elucidation, substrate recognition, binding and enzymatic repair, have contributed significantly to our understanding of this unique enzyme. Experimental studies have provided much needed thermodynamic, kinetic, and structural information, whereas computational studies have used these data to gain insight at the atomistic level and provided new information that could then inspire a new experimental study. Because of the relationship of the DNA photolyase to other important enzymes such as the 6−4 photolyase and cryptochrome,[6] it can be expected that this work will also impact these areas of current interest.

Acknowledgment. We gratefully acknowledge financial support of our work on the chemistry of radical ions by the National Institutes of Health (CA073775), the National Science Foundation (CHE-9733050 and CHE-0415344), and the Dreyfus Foundation for a Camille Dreyfus Teacher-Scholar Award to O.W. We also acknowledge a fruitful collaboration with the Walther Cancer Research Center at the University of Notre Dame and helpful comments by A. A. Stuchebrukhov and J. P. M. Schelvis.

References and Notes

(1) (a) Friedberg, E. C. *DNA Repair*; W. H. Freeman & Co.: New York, 1985; Chapters 1-5, 2-1, and 2-2. (b) Cadet, J.; Vigny, P. The Photochemistry of Nucleic Acids. In *Bioorganic Photochemistry Vol. I: Photochemistry and Nucleic Acids*; Morrison H., Ed.; Wiley & Sons: New York 1990; pp 53−100. (c) Fischer, G. J.; Johns, H. E. In *Photochemistry and Photobiology of Nucleic Acids Vol. I*; Wang, S. Y., Ed.; Academic Press: New York, 1976; pp 226−295. (d) Patrick, M. H.; Rahn, R. O. In *Photochemistry and Photobiology of Nucleic Acids Vol. I*; Wang, S. Y., Ed.; Academic Press: New York, 1976; Chapters D-1 and D-3, pp 35−95.

(2) (a) Taylor, J.-S. *Pure Appl. Chem.* **1995**, *67*, 183−190. (b) Taylor, J.-S. *Acc. Chem. Res.* **1994**, *27*, 76−82.

(3) (a) Li, Y. F.; Kim, S.-T.; Sancar, A. *Proc. Natl. Acad. Sci. U.S.A.* **1993**, *90*, 4389−4393. (b) Ley, R. D. *Proc. Natl. Acad. Sci. U.S.A.* **1993**, *90*, 4337.

(4) For reviews compare, e.g.: (a) Sancar, A.; Sancar, G. B. *Annu. Rev. Biochem.* **1988**, *52*, 29−67. (b) Sancar, A. *Biochemistry* **1994**, *33*, 2−9. (c) Sancar, A. In *Advances in Electron-Transfer Chemistry*; Mariano, P. S., Ed.; JAI Press: New York, 1992; Vol. 2, pp 215−272. (d) Begley, T. P. *Acc. Chem. Res.* **1994**, *27*, 394−401.

(5) (a) Begley, T. P. *Comput. Nat. Prod. Chem.* **1999**, *5*, 371−399. (b) Heelis, P. F.; Hartman, R. F.; Rose, S. D. *Chem. Soc. Rev.* **1995**, *24*, 289−297.

(6) (a) Deisenhofer J. *Mutat. Res.* **2000**, *460*, 143−149. (b) Sancar, A. *Chem. Rev.* **2003**, *103*, 2203−2238. (c) Sancar, A. *Adv. Protein Chem.* **2004**, *69*, 73−100.

(7) (a) Carell, T.; Burgdorf, L.; Butenandt, J.; Epple, R.; Schwogler, A. In *Bioorganic Chemistry*; Diederichsen, U., Ed.; Wiley-VCH: Weinheim, 1999; pp 337−345. (b) Carell, T.; Burgdorf, L. T.; Kundum L. M.; Cichon, M. *Curr. Opinion Chem. Biol.* **2001**, *5*, 491−498. (c) Weber, S.; *Biochim. Biophys. Acta* **2005** *1707*, 1−23.

(8) (a)Diogo, H.; Dias, A. R.; Dhalla, A.; Minas da Piedade, M.; Begley, T. P. *J. Org. Chem.* **1991**, *56*, 7340−7341. (b) Heelis, P. F.; Parsons, B. J. *J. Chem. Soc., Chem. Commun.* **1994**, *7*, 793−795.

(9) (a) Witmer, M. R.; Altmann, E.; Young, H.; Begley, T. P. *J. Am. Chem. Soc.* **1989**, *111*, 9264−9265. (b) McMordie, R. A. S.; Begley, T. P. *J. Am. Chem. Soc.* **1992**, *114*, 1886−1887.

(10) (a) Park, H.-W.; Kim, S.-T.; Sancar, A.; Deisenhofer, J. *Science* **1995**, *268*, 1866−1872. (b) Park, H.-W.; Sancar, A.; Deisenhofer, J. *J. Mol. Biol.* **1993**, *231*, 1122−1123.

(11) For studies of a simplified model, compare: Boussicault, F.; Krüger, O.; Wille, U. *Org. Biomol. Chem.* **2004**, *2*, 2742−2750.

(12) (a) Aida, M.; Kaneko, M.; Dupuis, M. *Intl. J. Quantum Chem.* **1996**, *57*, 949−957. (b) Rak, J.; Voityuk, A. A.; Rösch, N. *J. Phys. Chem A* **1998**, *102*, 7168−7175.

(13) (a) Rak, J.; Voityuk, A. A.; Rösch, N. *J. Mol. Stuct. (THEOCHEM)* **1999**, *488*, 163−168. Compare also: (b) Aida, M.; Inoue, F.; Kaneko, M.; Dupuis, M. *J. Am. Chem. Soc.* **1997**, *119*, 12274−12279.

(14) Voityuk, A. A.; Michel-Beyerle, M. E.; Rösch, N. *J. Am. Chem. Soc.* **1996**, *118*, 9750−9758.

(15) For an overview of the work in this area, see: Bally, T.; Borden W. T. *Rev. Comput. Chem.* **1999**, *13*, 1−71.

(16) Burdi, D.; Begley, T. P. *J. Am. Chem. Soc.* **1991**, *113*, 7768−7770.

(17) (a) Shafirovich, V.; Dourandin, A.; Geacintov, N. E. *J. Phys. Chem. B* **2001**, *105*, 8431−8435. (b) Weatherly, S. C.; Yang, I V.; Thorp, H. H. *J. Am. Chem. Soc* **2001**, *123*, 1236−1237. (c) Shafirovich, V.; Cadet, J.; Gasparutto, D.; Dourandin, A.; Huang, W.; Geacintov, N. E. *J. Phys. Chem. B* **2001**, *105*, 586−592. (d) Shafirovich, V.; Dourandin, A.; Huang, W.; Luneva, N. P.; Geacintov, N. E. *Phys. Chem. Chem. Phys.* **2000**, *2*, 4399−4408.

(18) Rak, J.; Voityuk, A. A.; Michel-Beyerle, M. E.; Rösch, N. *J. Phys. Chem. A* **1999**, *103*, 3569−3574.

(19) Hartman, R. F.; Van Camp, J. R.; Rose, S. D. *J. Org. Chem.* **1987**, *52*, 2684−2689.

(20) Heelis, P. F. *J. Mol. Model* **1995**, *1*, 18−21.

(21) Saettel, N. J. Dissertation, University of Notre Dame, 2002.

(22) (a) Scannell, M. P.; Yeh, S. R.; Falvey, D. E. *Photochem. Photobiol.* **1996**, *64*, 764−768. (b) Scannell, M. P.; Fenick, D. J.; Yeh, S.-R.; Falvey, D. E. *J. Am. Chem. Soc.* **1997**, *119*, 1971−1977.

(23) Kim, S.-T., Hartman, R. F.; Rose, S. D. *Photochem Photobiol.* **1990**, *52*, 789−794.

(24) Adman, E.; Jensen, L. H. *Acta Crystallogr. Sect B* **1970**, *26*, 1326−1334.

(25) Kleopfer, R.; Morrison, H. *J. Am. Chem. Soc.* **1972**, *94*, 255−264.

(26) Clark, T. A. *A Handbook of Computational Chemistry*; Wily & Sons: New York, 1985.

(27) Voityuk, A. A.; Rösch, N. *J. Phys. Chem. A* **1997**, *101*, 8335−8338.

(28) (a) Hendricks, J. H.; Lyapustina, S. A.; de Clercq, H. L.; Snodgrass, J. T.; Bowen, K. H. *J. Chem. Phys.* **1996**, *104*, 7788−7791. (b) Desfrancois, C.; Abdoul-Carime, H.; Khelifa, N.; Schermann, J. P. *Phys. Rev. Lett.* **1994**, *73*, 2436−2439. (c) Desfrancois, C.; Abdoul-Carime, H.; Schermann, J. P *J. Chem. Phys.* **1996**, *104*, 7792−7794. (d) Desfrancois, C.; Periquet, V.; Bouteiller, Y.; Schermann, J. P. *J. Phys. Chem. A* **1998**, *102*, 1274−1278. Aflatooni, K.; Gallup, G. A.; Burrow, P. D. *J. Phys. Chem. A* **1998**, *102*, 6205−6207.

(29) (a) Roehrig, G. H.; Oyler, N. A.; Adamowicz, L. *J. Phys. Chem.* **1995**, *99*, 14285−14289. (b) Smith, D. M. A.; Smets, J.; Elkadi, Y.; Adamowicz, L. *J. Phys. Chem. A* **1997**, *101*, 8123−8127. (c) Dolgounitcheva, O.; Zakrzewski, V. G.; Ortiz, J. V. *Chem. Phys. Lett.* **1999**, *307*, 220−226. (d) Russo, N.; Toscano, M.; Grand, A. *J. Comput. Chem.* **2000**, *21*, 1243−1250. (e) Wesolowski, S. S.; Leininger, M. L.; Pentchev, P. N.; Schaefer, H. F., III. *J. Am. Chem. Soc.* **2001**, *123*, 4023−4028. (f) Richardson, N. A.; Wesolowski, S. S.; Schaefer, H. F., III. *J. Am. Chem. Soc.* **2002**, *124*, 10163−10170.

(30) Schiedt, J.; Weinkauf, R.; Neumark, D. M.; Schlag, E. W. *Chem. Phys.* **1998**, *239*, 511−524.

(31) Desfracois, C.; Abdoul-Carime, H.; Schermann, J. P. *Int. J. Mod. Phys. B* **1996**, *10*, 1339−1395.

(32) Crawford, O. H.; Garrett, W. R. *J. Chem. Phys.* **1977**, *66*, 4968−4970.

(33) Wiley: J. R.; Robinson, J. M.; Ehdaie, S.; Chen, E. C. M.; Chen, E. S. D.; Wentworth, W. E.; *Biochem. Biophys. Res. Commun.* **1991**, *180*, 841−845.

(34) Aflatooni, K.; Gallup, G. A.; Burrow, P. D. *J. Phys. Chem. A* **1998**, *102*, 6205−6207.

(35) Huels, M. A.; Hahndorf, I.; Illenberger, E.; Sanche, L. *J. Chem. Phys.* **1998**, *108*, 1309−1312.

(36) (a) Smets, J.; McCarthy, W. J.; Adamowicz, L. *Chem. Phys. Lett.* **1996**, *256*, 360−369. (b) Smets, J.; Smith, D. M. A.; Elkadi, Y.; Adamowicz, L. *J. Phys. Chem. A* **1997**, *101*, 9152−9156. (c) Smets, J.; McCarthy, W. J.; Adamowicz, L. *J. Phys. Chem.* **1996**, *100*, 14655−14660. (d) Smets, J.; Smith, D. M. A.; Elkadi, Y.; Adamowicz, L. *J. Phys. Chem. A* **1997**, *101*, 9152−9156. (e) Dolgounitcheva, O.; Zakrzewski, V. G.; Ortiz, J. V. *J. Phys. Chem. A* **1999**, *103*, 7912−7917. (f) Smith, D. M. A.; Smets, J.; Adamowicz, L. *J. Phys. Chem. A* **1999**, *103*, 5784−5790. (g) Al-Jihad, I.; Smets, J.; Adamowicz, L. *J. Phys. Chem. A* **2000**, *104*, 2994−2998.

(37) Tantillo, D. J.; Chen, J. G.; Houk, K. N. *Curr. Opin. Chem. Biol.* **1998**, *2*, 743−750.

(38) Saettel, N. J.; Wiest, O. *J. Am. Chem. Soc.* **2001**, *123*, 2693−2694.

(39) McMordie, R. A. S.; Altmann, E.; Begley, T. P. *J. Am. Chem. Soc.* **1993**, *115*, 10370−10371.

(40) Durbeej, B.; Eriksson, L. A. *J. Am. Chem. Soc.* **2000**, *122*, 10126−10132.

(41) (a) Li, Y.-F.; Heelis, P. F.; Sancar, A. *Biochemistry* **1991**, *30*, 6322−6329. (b) Kim, S.-T.; Sancar, A.; Essenmacher, C.; Babcock, G. T. *Proc. Natl. Acad. Sci U.S.A.* **1993**, *90*, 8023−8027. (c) Aubert, C.; Vos, M. H.; Mathis, P.; Eker, A. P. M.; Brettel, K. *Nature* **2000**, *405*, 586−590.

(42) (a) Popović, D. M.; Zmiriæ, A.; Zariæ, S. D.; Knapp, E.-W. *J. Am. Chem. Soc.* **2002**, *124*, 3775−3782. (b) Cheung, M. S.; Daizadeh, Stuchebrukhov, A. A.; Heelis, P. F. *Biophys. J.* **1999**, *76*, 1241−1249.

(43) (a) Miki, K.; Tamada, T.; Nishida, H.; Inaka, K.; Yasui, A.; deRuiter, P. E.; Eker, A. P. M. *J. Mol. Biol.* **1993**, *233*, 167−169. (b) Tamada, T.; Kitadokoro, K.; Higuchi, Y.; Inaka, K.; Yasui, A.; De Ruiter, P. E.; Eker, A. P. M.; Miki, K. *Nature Struct. Biol.* **1997**, *4*, 887−891. (c) Komori, H.; Masui, R.; Kuramitsu, S.; Yokoyama, S.; Shibata, T.; Inoue, Y.; Miki, K. *Proc. Natl. Acad. Sci. U.S.A.* **2001**, *98*, 13560−13565.

(44) Mees, A.; Klar, T.; Gnau, P.; Hennecke, U.; Eker, A. P. M.; Carell, T.; Essen, L.-O. *Science* **2004**, *306*, 1789−1793.

(45) Hahn, J.; Michel-Beyerle, M. E.; Rösch, N. *J. Mol. Mod.* **1998**, *4*, 73−82.

(46) Hahn, J.; Michel-Beyerle, M. E.; Rösch, N. *J. Phys. Chem. B* **1999**, *103*, 2001−2007.

(47) Sanders, D. B.; Wiest, O. *J. Am. Chem. Soc.* **1999**, *121*, 5127−5134.

(48) (a) Antony J.; Medvedev. D. M.; Stuchebrukhov, A. A. *J. Am. Chem. Soc.* **2000**, *122*, 1057−1065. (b) Medvedev. D. M.; Stuchebrukhov, A. A. *J. Theor. Biol.* **2001**, *210* 237−248.

(49) Langenbacher, T.; Zhao, X.; Bieser, G.; Heelis, P. F.; Sancar, A.; Michel-Beyerle, M. E. *J. Am. Chem. Soc.* **1997**, *119*, 10532−10536.

(50) Weiner, S. J.; Kollman, P. A.; Case, D. A.; Singh, U. C.; Ghio, C.; Alagona, G.; Profeta, S.; Weiner, P. *J. Am. Chem. Soc.* **1984**, *106*, 765−784.

(51) (a) Weber, S.; Richter, G.; Schleicher, E.; Bacher, A.; Mobius, K.; Kay, C. W. M. *Biophys. J.* **2001**, *81*, 1195−1204. (b) Weber, S.; Mobius, K.; Richter, G.; Kay, C. W. M. *J. Am. Chem. Soc* **2001**, *123*, 3790−3798.

(52) Husain, I.; Sancar, G.; Holbrook, S.; Sancar, A. *J. Biol. Chem.* **1987** *262*, 13188−13197.

(53) Vande Berg, B. J.; Sancar, G. B. *J. Biol. Chem.* **1998**, *273*, 20276−20284.

(54) Torizawa, T.; Ueda, T.; Karamitsu, S.; Hitomi, K.; Todo, T.; Iwai, S.; Morikawa, K.; Shimada, I. *J. Biol. Chem.* **2004** *279*, 32950−32956.

(55) For recent reviews on the relationship of base flipping and DNA repair, compare: (a) Kunkel, T. A.; Wilson, S. H. *Nature* **1996**, *384*, 25−26. (b) Roberts, R. J. *Cell* **1995**, *82*, 9−12. (c) Vassylyev, D. G.; Morikawa,

K. *Curr. Opinion Struct. Biol.* **1997**, *7*, 103−109. (d) Roberts, R. J. Cheng, X. *Annu. Rev. Biochem.* **1998**, *67*, 181−198. (e) Lloyd, R. S.; Cheng, X. *Biopolymers*. **1997**, *44*, 139−51.

(56) E.g.: (a) Stivers, James T.; Drohat, Alexander C. *Arch. Biochem. Biophys.* **2001**, *396*, 1−9. (b) Cheng, X.; Roberts, R. J. *Nucl. Acid Res.* **2001**, *29*, 3784−3795.

(57) Katz, D. J.; Stuchebrukhov, A. A. *J. Chem. Phys.* **1998**, *109*, 4960−4970.

(58) Christine, K. S.; MacFarlane, A. W., IV; Yang, K.; Stanley, R. J. *J. Biol. Chem.* **2002**, *277*, 38229−38344. (b) Vande Berg, B. J.; Sancar, G. B. *J. Biol. Chem.* **1998**, *273*, 20276−20284.

(59) Butenandt, J., Burgdorf, L. T.; Carell, T. *Angew. Chem., Intl Ed. Engl.* **1999**, *38*, 708−711.

(60) MacFarlane IV, A. W.; Stanley, R. J. *Biochemistry* **2001**, *40*, 15203−15214.

(61) Ueda, T.; Kato, A.; Ogawa, Y.; Torizawa, T.; Kuramitsu, S.; Iwai, S.; Terasawa, H.; Shimada, I. *J. Biol.* Chem. **2004**, *279*, 52574−52579.

(62) Kim, S.-H.; Pearlman, D. A.; Holbrook, S. R.; Pirkle, D. *Molecular Basis of Cancer, Part A: Macromolecular Structure, Carcinogens and Oncogenes*; pp 143−152.

(63) Miaskiewicz, K.; Miller, J.; Cooney, M.; Osman, R. *J. Am. Chem. Soc.* **1996**, *118*, 9156−9163.

(64) Spector, T. I.; Cheatham, T. E., III; Kollmann, P. A. *J. Am. Chem. Soc.* **1997**, *119*, 7095−7104.

(65) Cornell, W. D.; Cieplak, P.; Bayly, C. I.; Gould, I. R.; Merz, K. M.; Ferguson, D. M.; Spellmeyer, D. C.; Fox, T.; Caldwell, J. W.; Kollman, P. A. *J. Am. Chem. Soc.* **1995**, *117*, 5179−5197.

(66) Rao, S. N.; Keepers, J. W.; Kollman, P. A. *Nucl. Acids Res.* **1984**, *11*, 4789−4807.

(67) Lavery, R.; Sklenar, H. *J. Biomol. Struct. Dyn.* **1988**, *6*, 63−91.

(68) Park, H.; Zhang, K.; Ren, Y.; Nadij, S.; Sinha, N.; Taylor, J.-S. *Proc. Natl. Acad. Sci U.S.A.* **2002**, *99*, 15965−15970.

(69) (a) McAteer, K.; Jing, Y.; Kao, J.; Taylor, J. S.; Kennedy, M. A. *J. Mol. Biol.* **1998**, *282*, 1013−1032. (b) Lee, J. H.; Choi, Y. J.; Choi, B. S. *Nucl. Acids Res.* **2000**, *28*, 1794−1801. (c) Husain, I.; Griffith, J.; Sancar, A. *Proc Natl Acad Sci U.S.A.* **1988**, *85*, 2558−25562. (d) Wang, C. I.; Taylor, J. S. *Chem. Res. Toxicol.* **1993**, *6*, 519−523. (e) Wang, C. I.; Taylor, J. S. *Proc. Natl. Acad. Sci. U.S.A.* **1991**, *88*, 9072−9076.

(70) Fuxreiter, M.; Luo, N. Jedlovszky, P.; Simon, I.; Osman, R. *J. Mol. Biol.* **2002**, *323*, 823−834.

(71) Vassylyev, D. G.; Kashiwagi, T.; Mikami, Y.; Ariyoshi, M.; Iwai, S.; Ohtsuka, E.; Morikawa, K. *Cell* **1995**, *83*, 773−782.